Division of Engineering
BROWN UNIVERSITY
PROVIDENCE, R. I.

ENGINEERING MATERIALS RESEARCH LABORATORY

EFFECT OF GAS DIFFUSION ON CREEP BEHAVIOR OF POLYCARBONATE

H. HOJO and W. N. FINDLEY

Materials Research Program
Brown University
ARPA SD-86

ARPA E-81
EMRL-51

April 1972

Effect of Gas Diffusion on Creep Behavior of Polycarbonate

Hidemitsu Hojo* and William N. Findley

Division of Engineering,
Brown University,
Providence, R.I.

Summary

Biaxial tension-tension creep experiments were performed to study the effect of gas diffusion on creep behavior of polycarbonate. Experiments were conducted on a thin-walled tubular specimen by applying both gas pressure and axial tension at room temperature, and measuring axial strain and gas absorption. It was found that the creep deformation was highly affected by the solubility controlled gas, carbon dioxide. The absorption measurements showed that the gas absorption behavior was clearly affected by the creep deformation of the material. Also an anomalous diffusion type behavior appeared even in permanent gas-polymer systems under creep conditions. The modified superposition principle satisfactorily predicted the recovery following creep. The axial creep for the biaxial tension-tension experiments were also computed from data previously reported for creep under combined tension and torsion of a different sample of polycarbonate.

*Present address: Department of Chemical Engineering, Tokyo Institute of Technology, Ookayama, Meguro-ku, Tokyo, Japan.

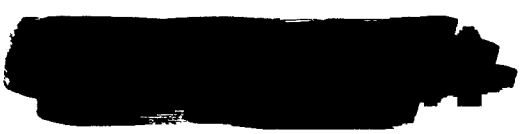

Introduction

A number of papers and data concerning the permeation of gases through plastic membranes [1-4]* and the penetration of organic vapors into polymers [1,5,6] have been published, but little information is available on the effect on creep of diffusing gases or vapors other than water vapor [7]. The permeation of gases and vapors through plastic materials is regarded as a combination of three processes, that is, as a process in which the gas first dissolves on one side of the material then diffuses through the material to the other side, and there evaporates out. For permanent gases, in general, their solubility is proportional to the partial pressure of the gas above the material, that is Henry's law, and the diffusion process obeys Fick's law. According to Fick's law, the rate of transfer of a diffusing substance through unit area of a section is proportional to the concentration gradient measured normal to the section. The proportionality constant is called the diffusion coefficient.

Therefore, the permeation of gases depends on both the diffusivity and the solubility of gases for the material. Thus the permeability equation is given by

$$Q = DS \frac{p_1 - p_2}{a} , \qquad (1)$$

where Q is the amount of gas passing through unit area per sec., D is the diffusion coefficient, S is the solubility coefficient and p_1 and p_2 are the partial pressures of the permeating gas at the two sides of the material of thickness a. It is known that the size of a gas molecule determines the diffusion rate. The solubility of the following gases is generally in the order of $CO_2 > O_2 > N_2 > H_2 > He$ for rubbers and plastics. But, gases such

---

*Numbers in square brackets refer to the references at the end of the paper.

as carbon dioxide do not always behave ideally in their dependence of solubility on pressure [8]. On the influence of straining [9,10], it was found that a considerable increase in permeability was effected by straining for polystyrene, polyethylene and polypropylene films, while polyethylene terephthalate and rubber films did not show this effect. However, there is no known information on the simultaneous behavior of both the creep of solid plastics and the diffusion of permanent gas into the material under relatively high pressure.

The objective of the present investigation is to obtain information on how an absorbed gas affects the creep behavior of plastics and how absorption is affected by creep deformation. For this purpose, biaxial creep testing was conducted on a thin-walled polycarbonate tube by applying both internal gas pressure and axial tensile load at room temperature and 50 per cent R.H..

Materials and Specimen

The polycarbonate employed in this investigation was from the same lot of material as that used in a previous study [11]. However, it was taken from an extruded plate instead of a rod and annealed in air instead of oil. This material, called Zelux, was produced by Westlake Plastics, and supplied by the Lawrence Radiation Laboratory. The intrinsic viscosities measured in methylene chloride for this material were about 0.50, implying a molecular weight of 25 to 30 x 10^3. The material was extruded as 2 by 10 inch bars. The specimen was cut parallel to the direction of extrusion and before final machining it was annealed in air. The annealing cycle was 9 hr. heating from 80°F to 260°F, held at 260°F for approximately 5 hr. and returned to 80°F over a 9 hr. period. Tensile strength of this type of material is about 8600 psi. Except for one test with Freon* all tests reported were performed on the same specimen. The

*The test with Freon was performed on the same specimen employed in [11].

specimen was machined and finished to the shape of a thin-walled tube with enlarged threaded ends. The overall length of the specimen was 8.0 in. and the gage length was 3.98 in. The average outside diameter of the test section was 0.9987 in. and the average wall thickness was 0.03929 in. The maximum deviation from the average thickness was 2 per cent. The specimen used in a preliminary test with Freon had an average wall thickness of 0.05975 in. The ends of the tube were sealed by end plugs and O-rings.

Experimental Apparatus

The creep testing machine employed for this investigation was the same as described in [12] except that no provision was made for torsion. It was equipped to subject a tubular specimen to combinations of tension and internal pressure as shown in Fig. 1. Crossed knife edge shackles were used at both ends of the specimen to achieve axial alignment. The knife edges were adjusted to minimize bending by using a special bending detector described in [12]. Axial strain was measured over a 4-inch gage length by means of an instrument employing a one-inch differential transformer and a matched transformer for reference [12]. The core of the reference transformer was adjusted to null balance by means of a micrometer screw which served as the strain read-out device. The sensitivity of strain measurement was 2.5×10^{-6} in/in.

The tests were performed in a room maintained at a temperature of 75 ± 0.5°F and 50 ± 1 per cent R.H. [13]. A thermal shield was placed around the specimen area to further reduce the temperature fluctuation.

Figure 2 shows the apparatus for gas pressure supply and control. The internal pressure was supplied from a gas cylinder A Fig. 2 to the inside of a specimen H through copper tubing F with connections of Sewagelok. Gas pressure was maintained constant with an accuracy of ± 0.2 psi. by means of a

pressure controller B during the test periods, and measured by use of a Heise gage P_3 Fig. 2. The gas flow volume was determined by using a U-tube C with a glass capillary D filled with machine oil.

Experimental Procedure

Gases used in this experiment were helium, air, nitrogen, carbon dioxide and Freon-22. Some properties of these gases are listed in Table I. The upper level of test pressure was chosen to be about 10 atm. This choice was consistent with industrial application and the properties of gases used.

The experimental procedure was as follows:

1. Before testing the air inside the tubing and specimen was replaced by the testing gas.
2. All valves were then closed and the gas pressure was regulated to a value nearly as high as the test pressure by a valve V_1.
3. Then V_2 was opened, gas was supplied to the system and then V_2 was closed again. The pressure was then maintained by controller B for 15 minutes or so before loading the specimen.
4. The internal pressure and tensile load were applied simultaneously, by opening V_4 and applying the required weights to a scale pan on the loading lever.
5. Immediately after loading the strain measurement was initiated and continued for two hours.
6. At 4.5 minutes after loading V_4 was closed and both V_5 and V_6 were opened to measure the gas flow volume.
7. After two hours under load the tensile load and the internal pressure were removed simultaneously. The pressure was released by closing V_5 and V_6 and then opening V_3 and V_4.

8. Strain readings were recorded during recovery at least until the strain approached the strain prior to the test within 20 x 10^{-6} in./in. for most tests.

It was observed that the final strain during recovery was often less then the final strain in the previous test. In some tests a positive strain greater than 20 x 10^{-6} in./in. remained. The positive strain remaining prior to the following tests was 60, 50, 80, 90, 35, 35, 40 x 10^{-6} in./in. for tests 4, 5, 17, 18, 20, 21, 23 respectively. Over the entire series of tests the specimen showed a shrinkage of 180 x 10^{-6} in./in..

In a preliminary experiment, a check was made of the effect on the axial strain of the heat generated by compressing the gas. The axial strain increased immediately after pressurization and then decreased gradually. It took about 30 to 40 minutes for the thermally induced strain to stabilize. For this reason, an aluminum cylinder with a diameter nearly equal to the bore of the specimen was inserted inside the specimen to quickly absorb the heat generated and reduce the volume of gas compressed, and hence the amount of heat generated.

Two overlapping series of tests were made. In one the circumferential principal stress σ_2 was constant at σ_2 = 1000 psi. while the axial principal stress σ_1 was changed so that σ_1/σ_2 = 1,2,3 respectively. In the other σ_1 was constant at σ_1 = 3000 psi. while σ_2 was changed such that σ_1/σ_2 = 1,2,3 respectively. The radial principal stress in all cases varied from a compression equal to the internal pressure at the inner surface to zero (atmospheric pressure) at the outer surface. The radial principal stress σ_3 at the inner surface for the first series was constant, σ_3 = -85.4 psi. In the second series the internal pressure (= $-\sigma_3$) was 85.4, 128.1 and 256.2 psi

for σ_1/σ_2 = 1,2,3 respectively (see Table II).

The equations used to determine the stresses were as follows:

$$\sigma_1 = \sigma_z + F/A \tag{2a}$$

$$\sigma_z = p(\pi d_i^2/4)/A \tag{2b}$$

$$\sigma_2 = \sigma_\theta = pd_i/2a \tag{2c}$$

$$A = \pi(d_o^2 - d_i^2)/4 \quad , \tag{2d}$$

where A = Sectional area, in.^{2}

d_i = Inside diameter, in.

d_o = Outside diameter, in.

p = Internal pressure, psi.

a = Thickness, in.

F = Axial load added, lb.

σ_z = Axial stress due to internal pressure, psi.

σ_θ = Circumferential stress due to internal pressure, psi.

σ_1 = Principal stress in axial direction, psi.

σ_2 = Principal stress in circumferential direction, psi.

The maximum stress level chosen, 3000 psi., corresponds to about 40% of the tensile strength of this material.

Results

Rectangular plots of axial creep strain versus time for different stress ratios and different gases are shown in Figs. 3 to 6.

In some curves such as Tests 2 and 11 in Fig. 3, Tests 12 and 21 in Fig. 4 and Tests 8, 9 and 10 in Fig. 5, the effect induced by the small

temperature spike resulting from compressing the gas is seen at just the initial stage of creep.

The creep was small in every case except that for carbon dioxide which was much greater than the creep for the other gases. Two tests were repeated after many intervening tests as shown in Figs.3 and 5. The agreement was excellent, especially for the last test number 22 as compared with the second test, see Fig. 3.

Discussion

In earlier work [14,15] it was shown that the creep behavior of many plastics under constant stress could be described quite well even for extended time periods by a power function of time such as

$$\varepsilon_{11} = \varepsilon_{11}^{o} + \varepsilon_{11}^{+} t^{n} \quad , \tag{3}$$

where ε_{11} is the total strain, ε_{11}^{o} is the instantaneous strain, t is the time, ε_{11}^{o} and ε_{11}^{+} are stress dependent functions, and n is a constant under isothermal conditions. Equation 3 may be written as follows:

$$\log (\varepsilon_{11} - \varepsilon_{11}^{o}) = \log \varepsilon_{11}^{+} + n \log t \quad . \tag{4}$$

This is an equation of a straight line in the variables $\log(\varepsilon_{11} - \varepsilon_{11}^{o})$ and $\log t$.

Some of the plots of $\log(\varepsilon_{11} - \varepsilon_{11}^{o})$ versus $\log t$ for the present experiments are shown in Fig. 7. Values of ε_{11}^{o} , ε_{11}^{+} and n determined from such straight line plots are listed in Table II for various gases and stress ratios. The results of the calculation using Eq. 3 are also shown as solid lines in Figs. 3 to 6.

Effect of Gas on Creep Behavior

Figure 8 shows the effect of gas on creep (total strain plotted) at a stress ratio σ_1/σ_2 of 3 (σ_2 = 1000 psi.). Also shown are data obtained from a test with Freon in a preliminary experiment using a different specimen. Figure 8 shows that the strains resulting from use of carbon dioxide and Freon are remarkably larger than those of the other gases. Also the strains for helium, air and nitrogen are nearly the same. Therefore, the creep behavior is highly affected by the solubility controlled gases, carbon dioxide and Freon, because of the plasticizing action of their dissolved gases. On the contrary, diffusion controlled gases like helium seem apparently to have little or no effect on the creep behavior. Concerning air and nitrogen, it is assumed that the diffusivity is far smaller than that of helium and the solubility is smaller than that of carbon dioxide [3]. In the case of Freon, it was observed that some of the pressurized Freon gas appeared to liquefy inside the tubular specimen.

Effect of Axial Stresses on Creep Behavior

In Fig. 9 the values of ε_{11}^{o}, ε_{11}^{+} and n are presented as a function of axial stress under a constant circumferential stress σ_2 = 1000 psi. (constant pressure). The instantaneous strain ε_{11}^{o} is almost the same level for different gases, but the lowest in helium gas. As expected it has a negative value at $\sigma_1 = 0$ because σ_2 = 1000 psi., not zero. Values of ε_{11}^{+} increase with increasing stress and show about the same level (except the highest stress point) for air, nitrogen and helium gases; but, they show much greater values for carbon dioxide. The values of n are different from gas to gas, especially at lower stresses, but again the value for carbon dioxide was markedly higher than for the other gases.

Effect of Internal Pressure on Creep Behavior

The effect of internal pressure, or circumferential stress σ_2, on values of ε_{11}^{o}, ε_{11}^{+} and n at a constant axial stress of σ_1 = 3000 psi. is given by Fig. 10. The values of ε_{11}^{+} increase with increasing pressure for both helium and carbon dioxide, but the value is much greater for carbon dioxide. The time exponent n shows different behaviors between dissolution controlled and diffusion controlled gases; n is much larger for carbon dioxide, a dissolution controlled gas.

Therefore, it is concluded that the dissolution controlled gases have a striking influence on the creep behavior of polycarbonate, but the creep behavior is not much influenced by the diffusion controlled gases. Also there is a pronounced effect of pressure on creep for carbon dioxide.

On the Absorbed Gas Volume

The absorption volumes of gases were observed instead of the permeation because of the experimental apparatus available. The results are shown in Figs. 11 and 12. The change in gas volume is given by the following relation:

$$W = W_1 + W_2 + W_3 + W_4 \quad , \tag{5}$$

where W = Total volume change at constant pressure observed, in.^{3}

W_1 = Volume change due to creep deformation, in.^{3}

W_2 = Volume absorbed into polymer, in.^{3}

W_3 = Volume permeated through polymer, in.^{3}

W_4 = Leakage gas volume, in.^{3}

Before and during creep testing, the leakage was checked by a detecting agent (detergent), and no leakage was found in any test, thus $W_4 = 0$.

Although W_2 and W_3 cannot be separated in our experiment, W_3 is assumed to be quite a small quantity or negligible for the short time of testing. The volume change due to creep W_1 can be calculated for two of the stress states $\sigma_1 = \sigma_2 = 1000$ psi. and $\sigma_1 = \sigma_2 = 3000$ psi. by assuming that the material behavior is isotropic and using the axial strain data ε_{11} for both axial and circumferential strain. For this case W_1 is given by the following,

$$W_1 = \frac{\pi}{4}(d + \Delta d)^2(\ell + \Delta\ell) - \frac{\pi}{4} d^2\ell \simeq \frac{3}{4}\pi d^2\ell\, \varepsilon_{11} , \qquad (6)$$

where d and ℓ are the inside diameter and length of the specimen tube respectively, Δd and $\Delta\ell$ are the change in diameter and length of the tube due to creep respectively and ε_{11} is the axial strain in a biaxial stress state for which $\varepsilon_{11} = \varepsilon_{22}$. The change in volume from the time of the first reading of gas volume ($t = 4.5$ min.) to two hours yields the following examples: for $\sigma_1 = \sigma_2 = 3000$ psi. W_1/W is 9.5, 2.4, 16.8 per cent for carbon dioxide, helium and air respectively; for $\sigma_1 = \sigma_2 = 1000$ psi. the corresponding values are 1.0, 1.0 and 11.8 per cent. For cases where the flow volume is small, but creep still important W_1/W may be larger. Since it is not possible to calculate W_1 for other stress states, since the above values of W_1/W are small and since the trends are clear without accounting for W_1, no correction has been made in the value of gas flow shown in Figs. 11 to 15 and identified as "apparent absorbed gas volume".

As described before, almost the same creep occured in air, nitrogen and helium (see Fig. 8), but a clear difference was found among the absorbed volumes of those gases (see Figs. 11 and 12). The order of increasing absorption corresponds to the inverse of increasing molecular size (except for carbon dioxide). Helium with the smallest molecular diameter diffuses through

the intermolecular space of the polymer easily, so it shows a large amount of absorbed volume. Owing to the inclusion of oxygen in air, the absorbed volume of air is larger than that of nitrogen, since the molecular diameter of oxygen is less than nitrogen.

The effect of stress state is shown in Fig. 13, where the apparent gas volume absorbed at two hours versus axial stress σ_1 at constant pressure for various gases is given. For this comparison all volumes have been adjusted to 0°C and one atmosphere of pressure. At constant pressure, though the effect of axial stress σ_1 on the gas absorption is not great, the volumes of helium and air show an increasing tendency and those of carbon dioxide and nitrogen show a decreasing tendency with increasing axial stress σ_1. Those tendencies are similar to those of the time exponent n, except for air, as shown in Fig. 9.

The strong effect of pressure (or circumferential stress) on absorbed gas is evident in Fig. 14. For this comparison all volumes have been adjusted to 0°C and one atmosphere of pressure. The absorption increases with increasing pressure for all gases but the tendency is opposite between carbon dioxide versus helium or air or nitrogen.

In the case of dissolution controlled gas, the absorption is considered to take place by ordinary dissolution and "hole-filling" processes [8]. Increasing the axial stress from σ_1 = 1000 psi toward 3000 psi while holding the circumferential stress constant at σ_2 = 1000 psi as in Fig. 13 would change the shape of strain induced molecular spacing from circular to elongated-slit type while reducing the minimum width of the hole. In such circumstances, therefore, the pre-existing holes large enough to accommodate and to disperse the penetrant molecules would reduce, so the effect of the change in the shape of strain alone would result in a decrease in absorption with increase in axial stress as shown for carbon dioxide and nitrogen in Fig. 13 but not for helium and air. The change in absorbed volume shown in Fig. 13 for nitrogen, air and

helium are quite small, however.

Increasing the circumferential stress for σ_2 = 1000 toward 3000 psi. holding the axial stress constant as in Fig. 14 would change the shape of the strain induced molecular spacing from an elongated-slit to a circular shape while increasing the minimum dimension. Thus the absorption would increase as shown in Fig. 14. However, in Fig. 14 there is another factor which is much more important in increasing the absorption, that is, the pressure also increased. Although Henry's law is obeyed only over the pressure range 0 - 1.0 atm for various gases [8], the dissolution process strongly depends on pressure and the permeation process also depends on pressure.

The diffusion coefficient is known to react exponentially to change in the apparent free volume, and Yasuda et al. [10] proposed the following relationship between diffusion coefficient D and strain ε :

$$D(\varepsilon) = D(0)\exp\left\{\frac{V^*}{V_f(0)}\left[\frac{V_f(\varepsilon) - V_f(0)}{V_f(\varepsilon) + V_f(0)}\right]\right\} , \qquad (7)$$

where $V_f = V - V_o$, V_f is the free volume in the material, V^* the characteristic volume required to accommodate the diffusing gas molecule in the material, V the specific volume, and V_o the extrapolated value of V at 0°K . Therefore, the increase in absorbed volume for the diffusion controlled helium may be explained by an increase in free volume in the material due to the creep deformation.

Filled circles in Figs. 13 and 14 indicate corrections for volume increase due to creep deformation, assuming that the axial strain and circumferential strain take the same value when the stress ratio is unity.

To check the behavior of gas absorption in the polymer, a further analysis was made. In organic vapor penetrant-polymer systems, when the diffusion is of the Fickian type, the absorption of the penetrant is initially proportional to the square root of the time, provided that a steady surface equilibrium is established immediately and that the diffusion coefficient is a constant. In this case, the equation for absorption is given by the following:

$$\frac{M_t}{M_\infty} = \frac{4}{\pi}\left(\frac{Dt}{a^2}\right)^{1/2} , \qquad (8)$$

where M_t = Amount of diffusing gas taken up by the material in a time t,

M_∞ = Equilibrium absorption,

D = Diffusion coefficient,

a = Thickness of the material.

Plots of the apparent absorbed volume versus $\sqrt{t}$ are shown in Fig. 15. The data for carbon dioxide is a straight line on Fig. 15. Thus it is in very good agreement with (8). This indicates that the diffusion of carbon dioxide is of the Fickian type. Helium is nearly straight but shows a slight sigmoid character -- so nearly Fickian. However, nitrogen and air have an irregular, roughly sigmoidal shape, characteristic of anomalous or non-Fickian diffusion. Non-Fickian diffusion is found in organic vapor-polymer systems under the glass transition temperature. Generally, the anomalous behavior is explained as the combined effects of time or history, molecular orientation and internal stress on both the diffusion coefficient and on the surface concentration. In the first stage of two-stage absorption, vapor is absorbed until quasi-equilibrium is established at the surface of the polymer, then the equilibrium spreads throughout the polymer. Absorption in the second stage proceeds by a slow increase of the quasi-equilibrium throughout the material.

Thus anomalous-diffusion like behavior appears even in the permanent gas-polymer system under creep conditions when subjected to relatively high gas pressure.

Creep Recovery

Creep recovery was measured after the two hour loading period. In air, nitrogen, and helium, the deformation due to creep was fully recovered within twenty or thirty hours, while for carbon dioxide there remained a large amount of strain induced by the dissolution of the gas. It turned out, however, that this permanent set was only apparent, because it recovered completely by applying air pressure for a long duration of time.

When the pressure was released after the creep test using Freon in the preliminary experiment the specimen was found to have a clouded appearence and an inner layer of material a few thousands in. thick was completely separated from the specimen. This action presumably resulted from the following causes. The plasticizing action of the dissolved Freon reduced the van der Waals forces and hence reduced the strength of the polymer where the concentration of Freon was the highest. On release of pressure the large size of the Freon molecule impeded its diffusion out of the polymer. Thus the vapor pressure of Freon at 1 atm apparently exceeded the reduced strength of the polymer.

In [16] it was shown that the superposition principle was useful in predicting recovery following creep at constant stress even after long time. For recovery strain ε_R, after removal of load at time t_R, the following equation is obtained from (3) by using superposition,

$$\varepsilon_R = \varepsilon_{11}^{+} [t^n - (t - t_R)^n] \quad , \qquad t > t_R \quad , \qquad t_R = 2 \text{ hours} \quad . \tag{9}$$

The recovery strain following creep was calculated from the creep constants in Table II with this equation as shown in Fig. 16, together with the test data. The agreement between theory and data is excellent for helium, air and nitrogen, and rather good for carbon dioxide.

Prediction from Combined Tension-Torsion Creep

From the results of combined tension-torsion creep of polycarbonate by Lai and Findley [11] it is possible to calculate the creep behavior under tension and internal pressure, assuming the material is isotropic. The general equation is given in [17]. From the general equation the expression for axial strain ε_{11} in tubes subjected to axial stress σ_1, and circumferential stress σ_2 can be expressed as follows.

$$\varepsilon_{11} = \pi_1(\sigma_1 + \sigma_2) + \pi_2(\sigma_1^2 + \sigma_2^2) + \pi_3(\sigma_1 + \sigma_2)^2 + \pi_4(\sigma_1 + \sigma_2)(\sigma_1^2 + \sigma_2^2)$$
$$+ \pi_5(\sigma_1 + \sigma_2)^3 + \sigma_1[\nu_o + \nu_1(\sigma_1 + \sigma_2) + \nu_2(\sigma_1^2 + \sigma_2^2)$$
$$+ \nu_3(\sigma_1 + \sigma_2)^2] \quad , \qquad (10)$$

where the coefficients $\pi_1 \ldots, \nu_o \ldots$ are functions of time and properties of material. Values of $\pi_1 \ldots, \nu_o \ldots$ determined from a different specimen of polycarbonate as reported in [11] are shown in Table III.

Using (10) and the constants in Table III obtained from combined tension-torsion creep of a different sample of polycarbonate equations for creep corresponding to the present series of creep tests using air pressure were calculated. The constants for the resulting equations are shown in Table IV together with the constants for the corresponding equation for axial creep determined from the present series of creep experiments using air pressure. The strain at one hour in the present tests was substantially greater than the predicted strain.

This was generally true of ε_{11}^{o} and n also, but for ε_{11}^{+} the predicted values were usually larger than the results of the present experiments. However, when σ_2 was increasing with constant σ_1 the trend of ε_{11}^{+} from the present tests was opposite to the predicted trend as shown in Table IV. These differences may result from the difference in the extrusion and heat treatment of the two samples.

Acknowledgment

This investigation was performed under the auspices of the Advanced Research Projects Agency of the Department of Defense [Materials Science Research Program (SD-86)]. The authors are indebted to Messrs. R. M. Reed and J. F. Tracy and Dr. J. S. Y. Lai for valuable assistance in performing the experiments and to Miss L. L. Bassett for typing the manuscript.

References

1) Crank, J. and Park, G. S., ed., "Diffusion in Polymers," Academic Press (1968).

2) Doty, P. M., "On the Diffusion of Vapors Through Polymers," J. Chem. Phys., 14, 244 (1946).

3) Van Amerongen, G. J., "Influence of Structure of Elastomers on Their Permeability to Gases," J. Polym. Sci., 5, 307 (1950).

4) Waack, R., Alex, N. H., Frisch, H. L., Stannett, V. and Szwarc, M., "Permeability of Polymer Film to Gases and Vapors," Ind. Eng. Chem., 47, 2524 (1955).

5) Crank, J., "A Theoretical Investigation of the Influence of Molecular Relaxation and Internal Stress on Diffusion in Polymers," J. Polym. Sci., 11, 151 (1953).

6) Newns, A. C., "The Sorption and Desorption Kinetics of Water in a Regenerated Cellulose," Trans. Faraday Soc., 52, 1533 (1956).

7) Yamamura, H. and Kuramoto, N., "Diffusion-Controlled Mechanical Properties of Polyvinyl Alcohol and Polyvinyl Formals," J. Appl. Polym. Sci., 2, 71 (1959).

8) Michaels, A. S., Vieth, W. R. and Barrie, J. A., "Solution of Gases in Polyethylene Terephthalate," J. Appl. Phys., 34, 1 (1963).

9) Rosen, B., "Time-Dependent Tensile Properties. Part II: Porosity of Deformed Glasses," J. Polym. Sci., 47, 19 (1960).

10) Yasuda, H., Stannett, V., Frisch, H. L. and Peterlin, A., "The Permeability of Strained Polymer Films," Makromolek. Chem., 73, 188 (1964).

11) Lai, J. S. Y. and Findley, W. N., "Combined Tension-Torsion Creep Experiments on Polycarbonate in the Nonlinear Range," Polym. Eng. and Sci., 9, 378 (1969).

12) Findley, W. N. and Gjelsvik, A., "A Biaxial Testing Machine for Plasticity, Creep, or Relaxation under Variable Principal-Stress Ratios," Proc. ASTM, 62, 1103 (1962).

13) Findley, W. N and Reed, R. M., "A Constant Temperature and Humidity Room," ASHRAE Journal, April, 45 (1970).

14) Findley, W. N., "Creep Characteristics of Plastics," Symposium on Plastics, ASTM, 118 (1944).

References (cont'd)

15) Findley, W. N., "Prediction of Performance of Plastics under Long-Term Static Loads," Trans. Plastics Inst., London, 30, No. 87, 138 (1962).

16) Findley, W. N. and Peterson, D. B., "Prediction of Long-Time Creep with Ten-Year Creep Data on Four Plastic Laminates," Proc. ASTM, 58, 841 (1958).

17) Onaran, K. and Findley, W. N., "Combined Stress Creep Experiments on a Nonlinear Viscoelastic Material to Determine the Kernel Functions for a Multiple Integral Representation of Creep," Trans. Soc. of Rheology, 9, 299 (1965).

Table I: Properties of Gases Used*

Type of gas	Molecular Weight	Molecular diameter (Å)	Polarity	Density 0°C, 1 atm (g/ℓ)	Boiling Point (°C)	Viscosity 20°C, 1 atm (poise)
Freon-22 ($CHClF_2$)	86.48	-	Polar	1.4909 (-69°C)	- 39.8	**1.28×10^{-4}
Carbon dioxide (CO_2)	44.01	3.34	Polar	1.977	- 78.5	1.48×10^{-4}
Air	**28.97	2.98(O_2)	Non-Polar	1.2929	-194.5	1.83×10^{-4} (18°C)
Nitrogen (N_2)	28.01	3.15	Non-Polar	1.2506	-195.8	1.78×10^{-4} (27.4°C)
Helium (He)	4.0026	1.90	Non-Polar	0.1785	-268.9	1.94×10^{-4}

* Weast, R. C., ed.: "Handbook of Chemistry and Physics," 48th ed., The Chemical Rubber Pub. Co., Cleveland (1967-68).

** These values are from another source.

Table II: Evaluation of ε_{11}^{o} , ε_{11}^{+} and n in Eq. 3

σ_1 psi	σ_2 psi	Gas	Test No.	$\varepsilon_{11} = \varepsilon_{11}^{o} + \varepsilon_{11}^{+} t^{n}$ Percent
3000	0	-	1	$0.8700 + 0.0655\ t^{0.102}$
1000	1000	He	8	$0.1830 + 0.0094\ t^{0.142}$
		Air	6	$0.1840 + 0.00975\ t^{0.213}$
		N_2	21	$0.1855 + 0.0083\ t^{0.340}$
		CO_2	17	$0.1875 + 0.0408\ t^{0.451}$
2000	1000	He	18	$0.4740 + 0.0226\ t^{0.145}$
		Air	11	$0.4760 + 0.0205\ t^{0.199}$
		N_2	12	$0.4770 + 0.0194\ t^{0.242}$
		CO_2	13	$0.4800 + 0.0560\ t^{0.437}$
3000	1000	He	9	$0.7750 + 0.0400\ t^{0.153}$
		Air	22	$0.7760 + 0.0415\ t^{0.176}$
		N_2	20	$0.7650 + 0.0540\ t^{0.126}$
		CO_2	15	$0.7920 + 0.0792\ t^{0.398}$
3000	1500	He	19	$0.7230 + 0.0406\ t^{0.145}$
		Air	14	$0.7230 + 0.0437\ t^{0.163}$
		N_2	-	-
		CO_2	23	$0.7300 + 0.0996\ t^{0.397}$
3000	3000	He	5	$0.5300 + 0.0620\ t^{0.0597}$
		Air	4	$0.5570 + 0.0356\ t^{0.202}$
		N_2	7	$0.5550 + 0.0353\ t^{0.163}$
		CO_2	16	$0.5685 + 0.1335\ t^{0.450}$

Table III: Time and Material Functions from Reference [11] for Eq. 10

$$\pi_1 = -1.225 \times 10^{-6} - 0.074 \times 10^{-6}\, t^{0.15}$$

$$\pi_2 = +0.015 \times 10^{-9}$$

$$\pi_3 = -0.031 \times 10^{-9} + 0.04 \times 10^{-9}\, t^{0.15}$$

$$\pi_4 = -0.004 \times 10^{-12} - 0.009 \times 10^{-12}\, t^{0.15}$$

$$\pi_5 = -0.0005 \times 10^{-12} - 0.002 \times 10^{-12}\, t^{0.15}$$

$$\nu_o = 4.03 \times 10^{-6} + 0.21 \times 10^{-6}\, t^{0.15}$$

$$\nu_1 = 0.016 \times 10^{-9} - 0.04 \times 10^{-9}\, t^{0.15}$$

$$\nu_2 = 0.013 \times 10^{-12} + 0.013 \times 10^{-12}\, t^{0.15}$$

$$\nu_3 = -0.0025 \times 10^{-12} + 0.005 \times 10^{-12}\, t^{0.15}$$

Table IV: Prediction from Combined Tension - Torsion Creep in Air

Stress (psi)			ε_{11}^{o}	ε_{11}^{+}	$\varepsilon_{11} = \varepsilon_{11}^{o} + \varepsilon_{11}^{+} t^{n}$	n
σ_1	σ_2		%	%	at t = /hr.	
3000	0	Predicted	0.8577	0.0597	0.9174	0.15
		Tested	0.8700	0.0655	0.9355	0.102
3000	1000	Predicted	0.7114	0.0636	0.7750	0.15
		Tested	0.7760	0.0415	0.8175	0.176
3000	1500	Predicted	0.6373	0.0672	0.7045	0.15
		Tested	0.7230	0.0437	0.7667	0.163
3000	3000	Predicted	0.4074	0.0744	0.4818	0.15
		Tested	0.5570	0.0356	0.5926	0.202
2000	1000	Predicted	0.4289	0.0349	0.4638	0.15
		Tested	0.4760	0.0205	0.4965	0.199
1000	1000	Predicted	0.1514	0.0136	0.1650	0.15
		Tested	0.1840	0.00975	0.1938	0.213

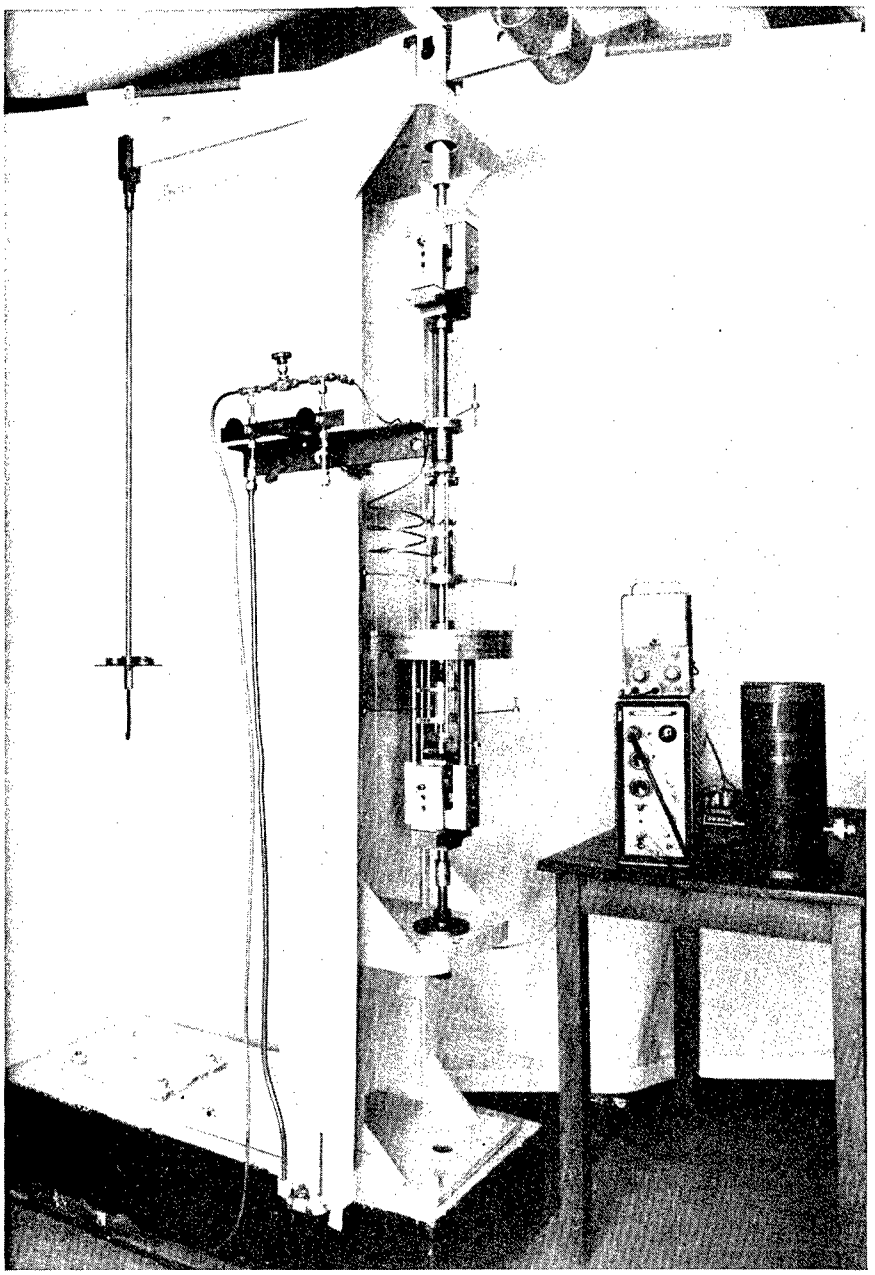

Fig. 1. Apparatus for Creep of Tubular Specimens under Tension and Internal Pressure

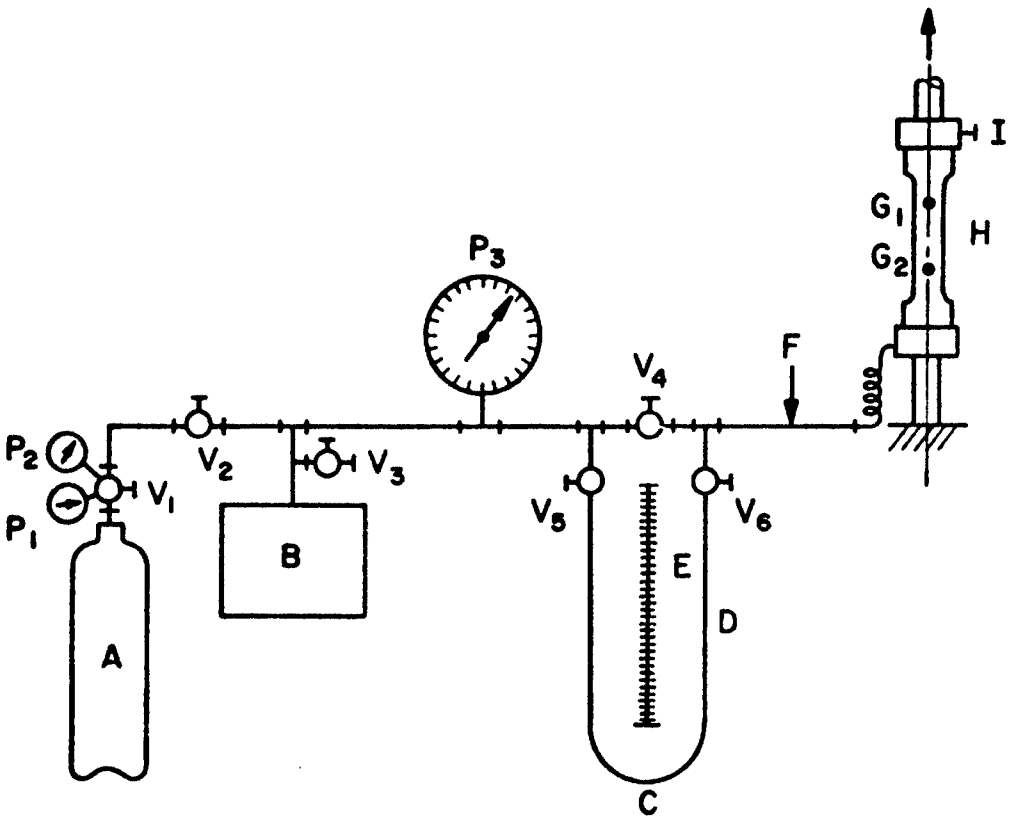

Fig. 2. Apparatus for Gas Pressure Supply and Control

A. Gas container

B. Pressure controller

C. U-tube

D. Glass capillary

E. Scale

F. Copper tubing

G_1,G_2. Gage section of tubular test specimen

H. Tubular specimen

I,V_3. Gas purging valves

P_1,P_2,P_3. Bourdon gages

V_1. Pressure regulating valve

V_2-V_6. Valves

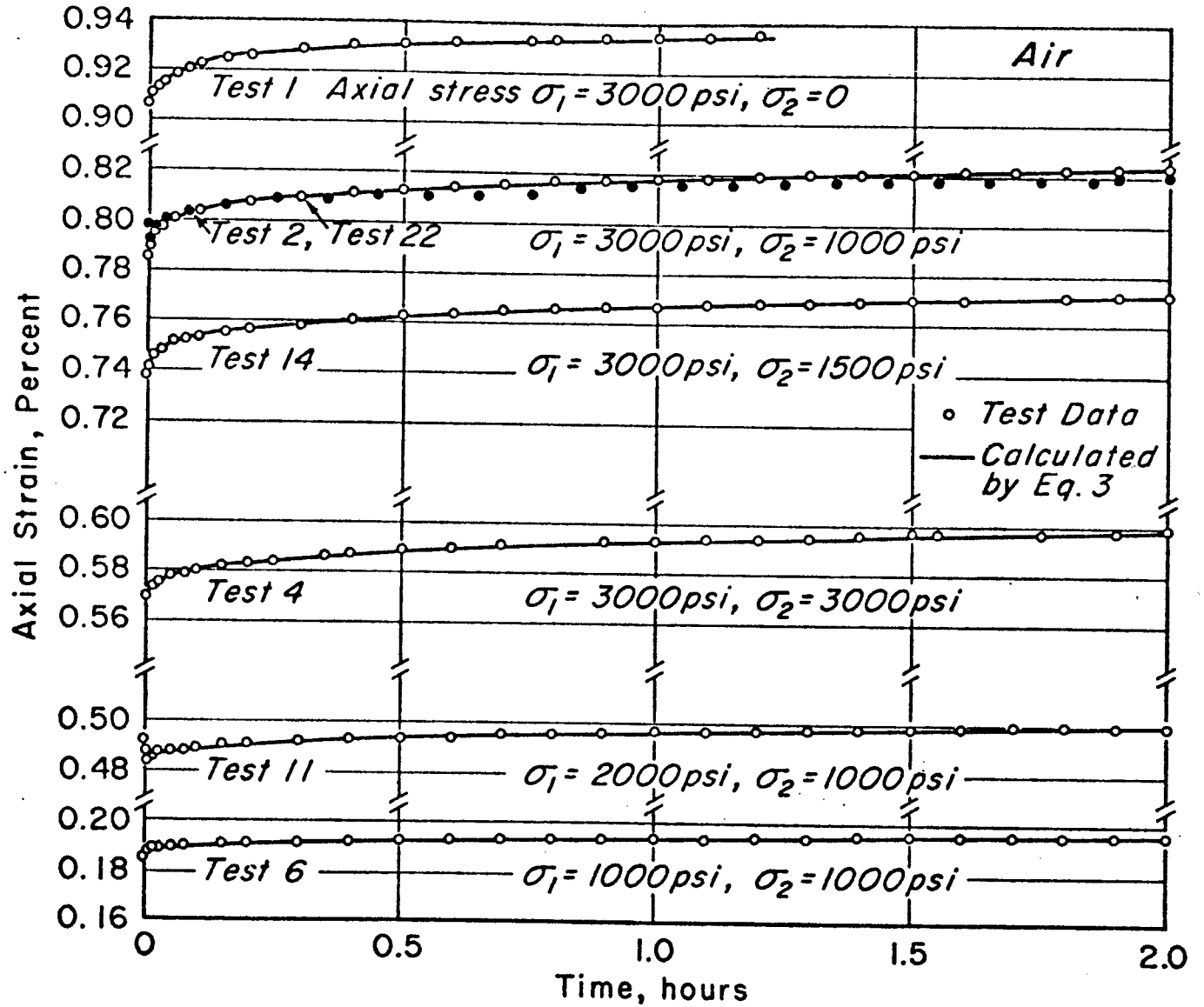

Fig. 3. Creep Curves for Polycarbonate Tubes Pressurized by Air at Various Stresses, 75°F and 50 per cent Relative Humidity

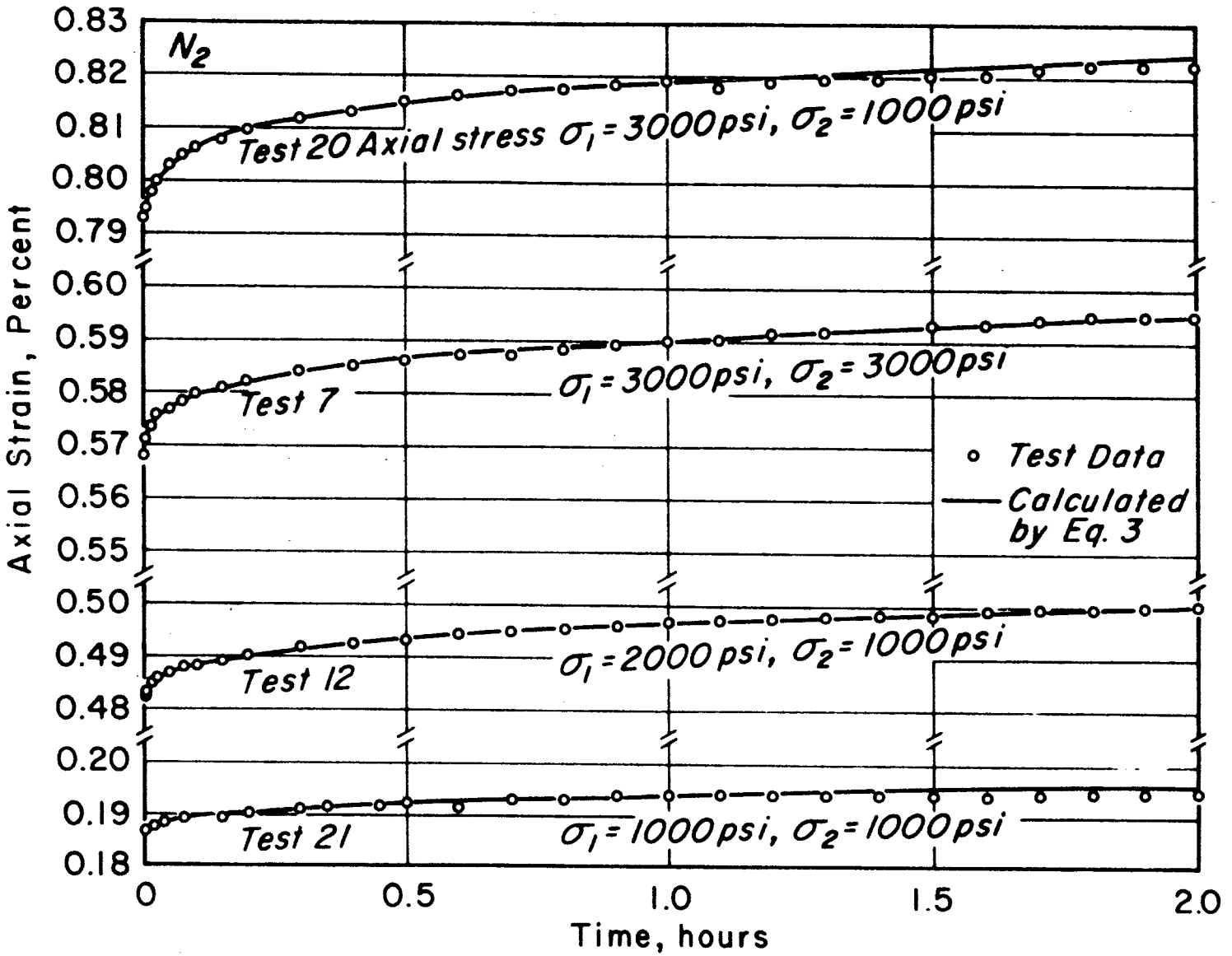

Fig. 4. Creep Curves for Polycarbonate Tubes Pressurized by Nitrogen at Various Stresses, 75°F and 50 per cent Relative Humidity

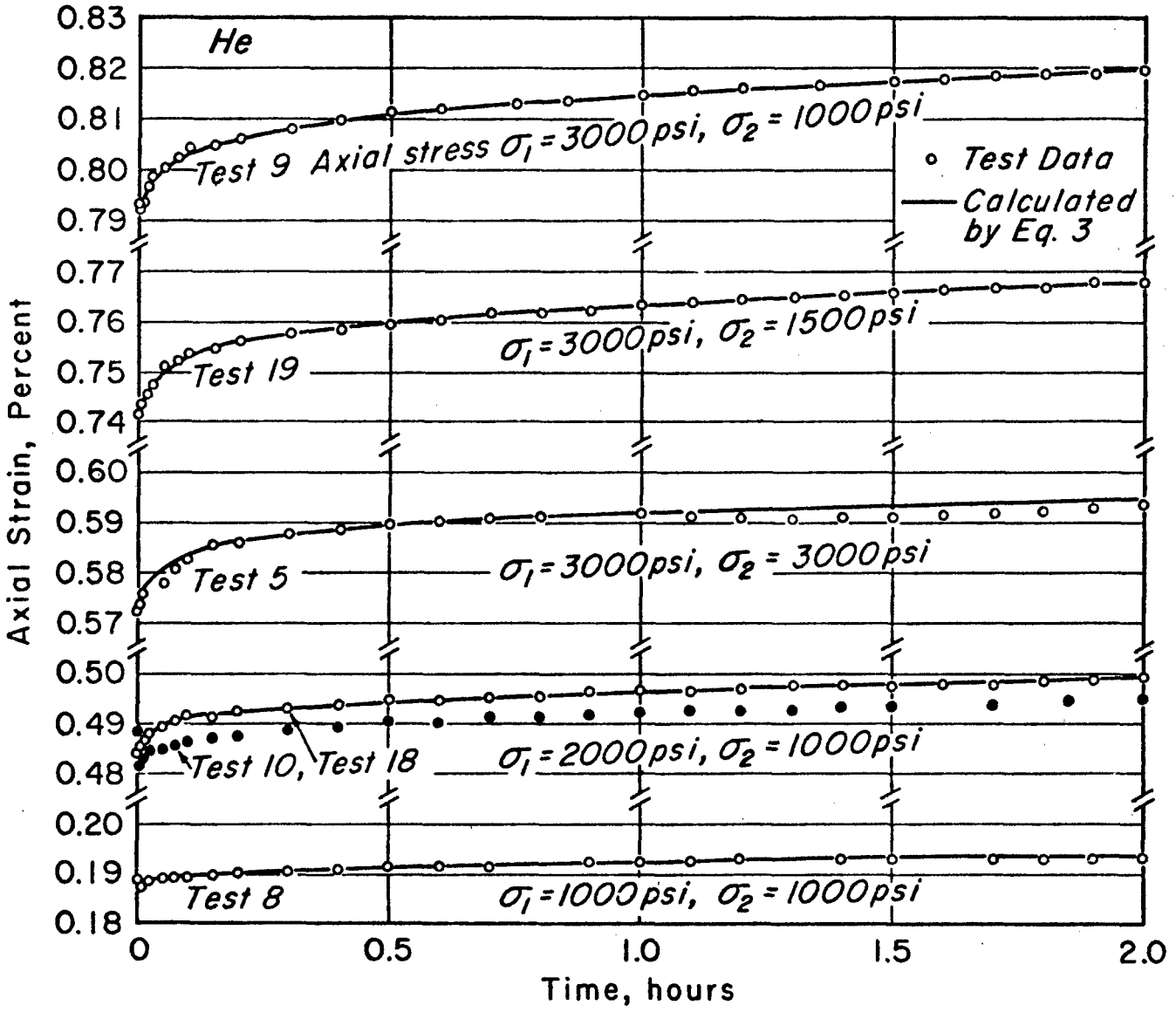

Fig. 5. Creep Curves for Polycarbonate Tubes Pressurized by Helium at Various Stresses, 75°F and 50 per cent Relative Humidity

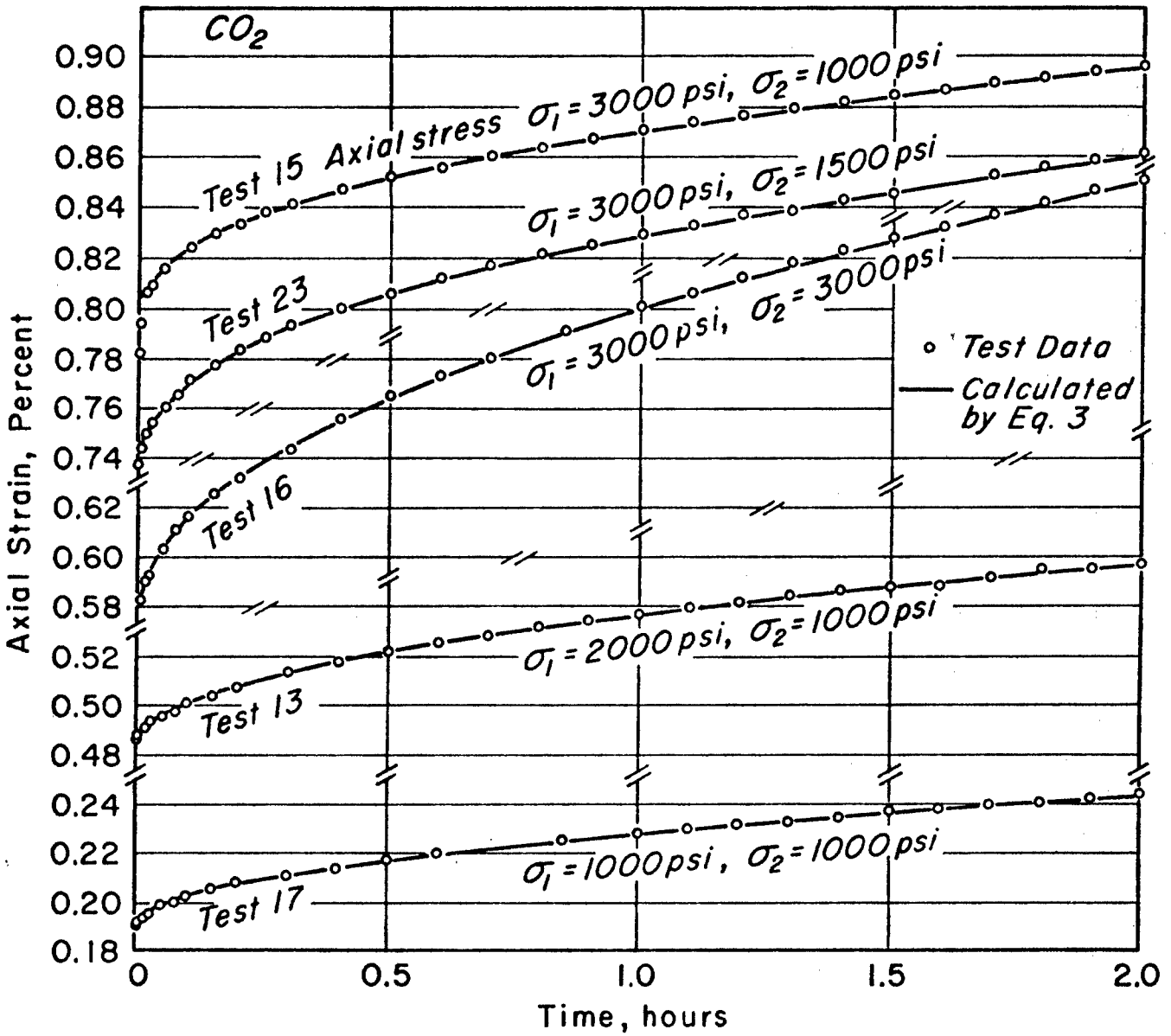

Fig. 6. Creep Curves for Polycarbonate Tubes Pressurized by Carbon Dioxide at Various Stresses, 75°F and 50 per cent Relative Humidity

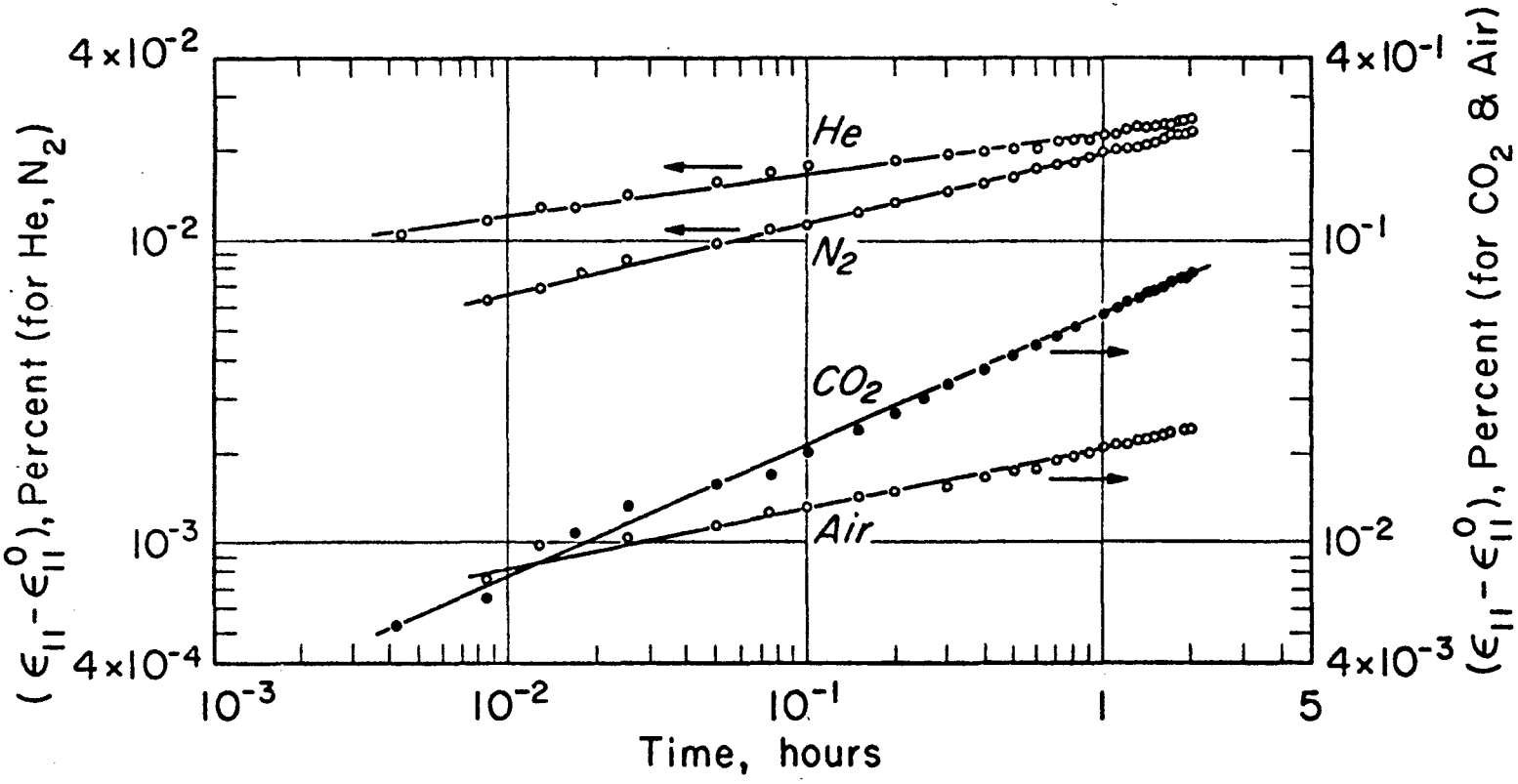

Fig. 7. Log-log Plots of Strain Difference vs. Time for Axial Tensile Creep at $\sigma_1/\sigma_2 = 2$ (σ_1 = 2000 psi, σ_2 = 1000 psi)

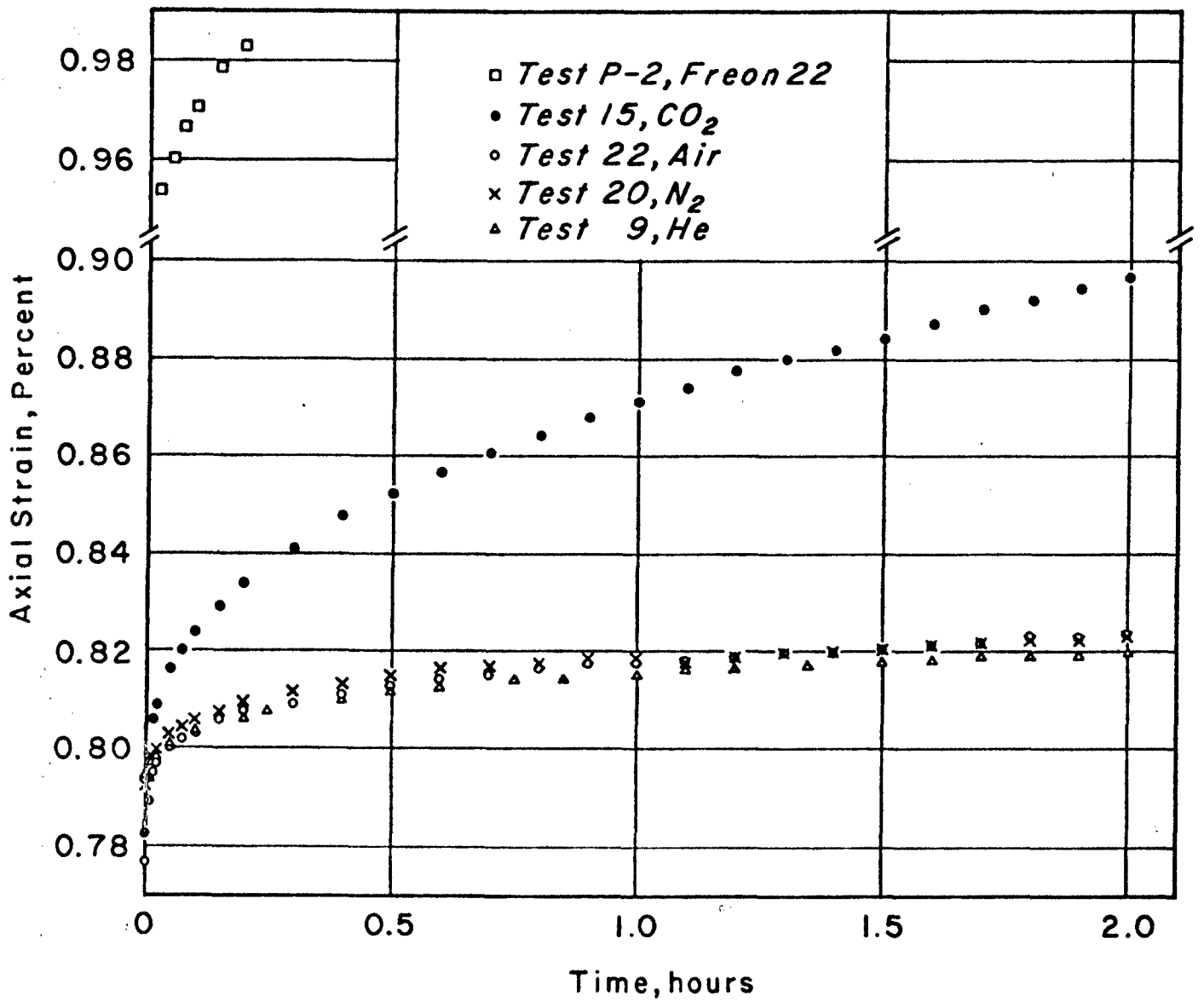

Fig. 8. Effect of Gases on Creep at $\sigma_1/\sigma_2 = 3$ (σ_1 = 3000 psi, σ_2 = 1000 psi)

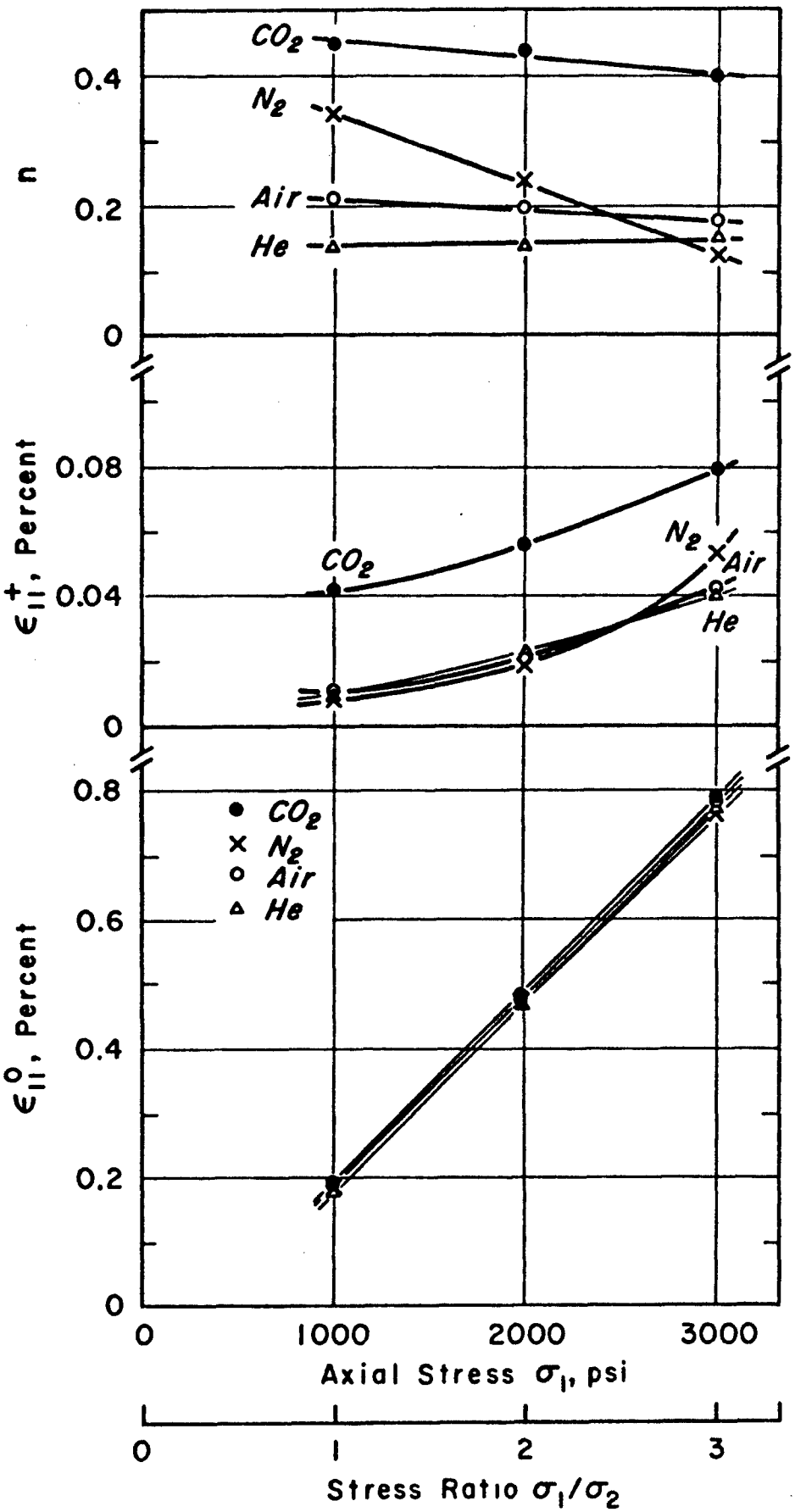

Fig. 9. Relationship Between $\epsilon_{11}^{o}, \epsilon_{11}^{+}$ and n in Eq. 3 and Axial Stress σ_1 for a Constant Value of σ_2 = 1000 psi

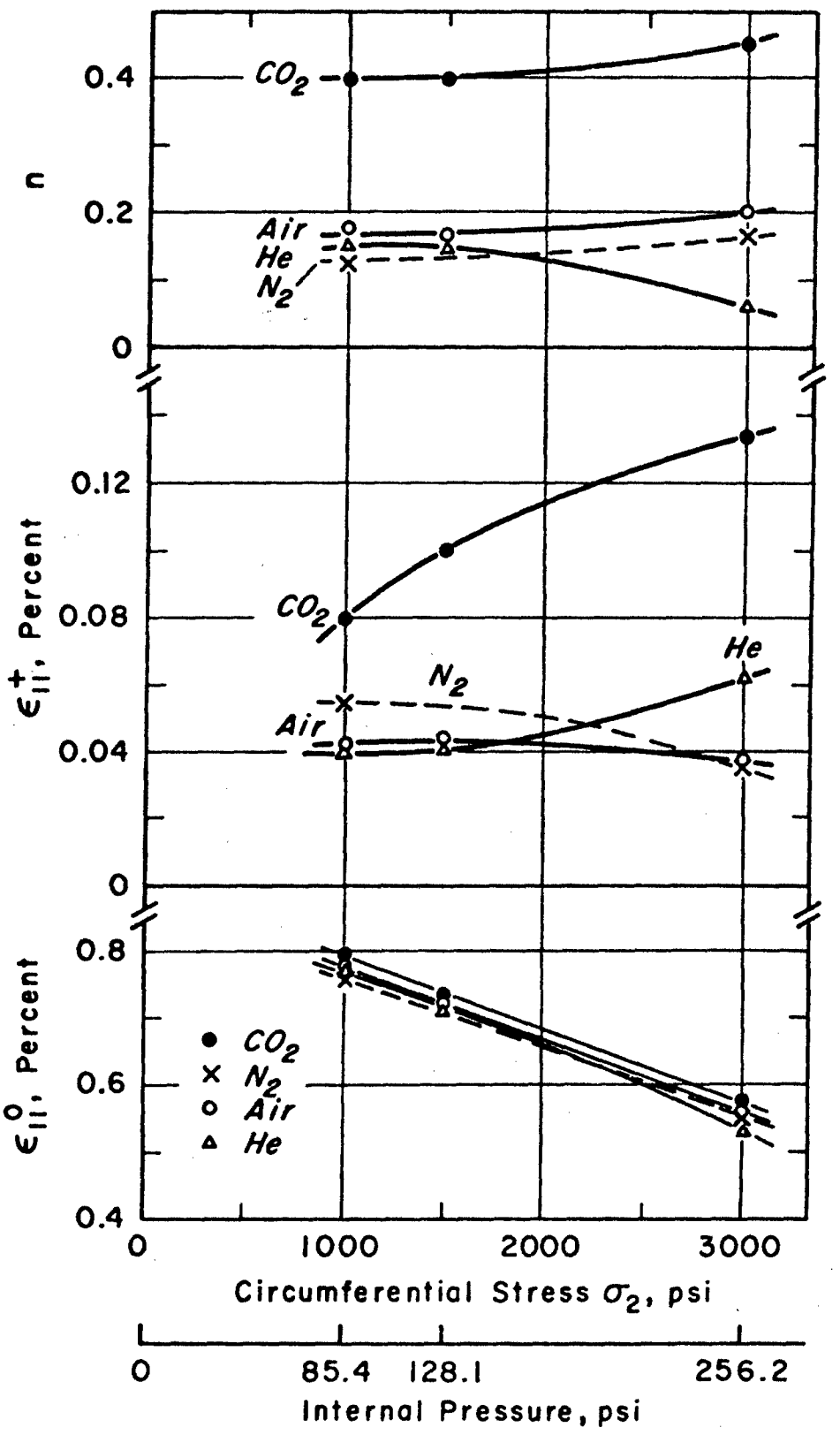

Fig. 10. Relationship Between $\epsilon_{11}^o, \epsilon_{11}^+$ and n in Eq. 3 and Circumferential Stress σ_2 (or internal pressure) at Constant Axial Stress σ_1 = 3000 psi

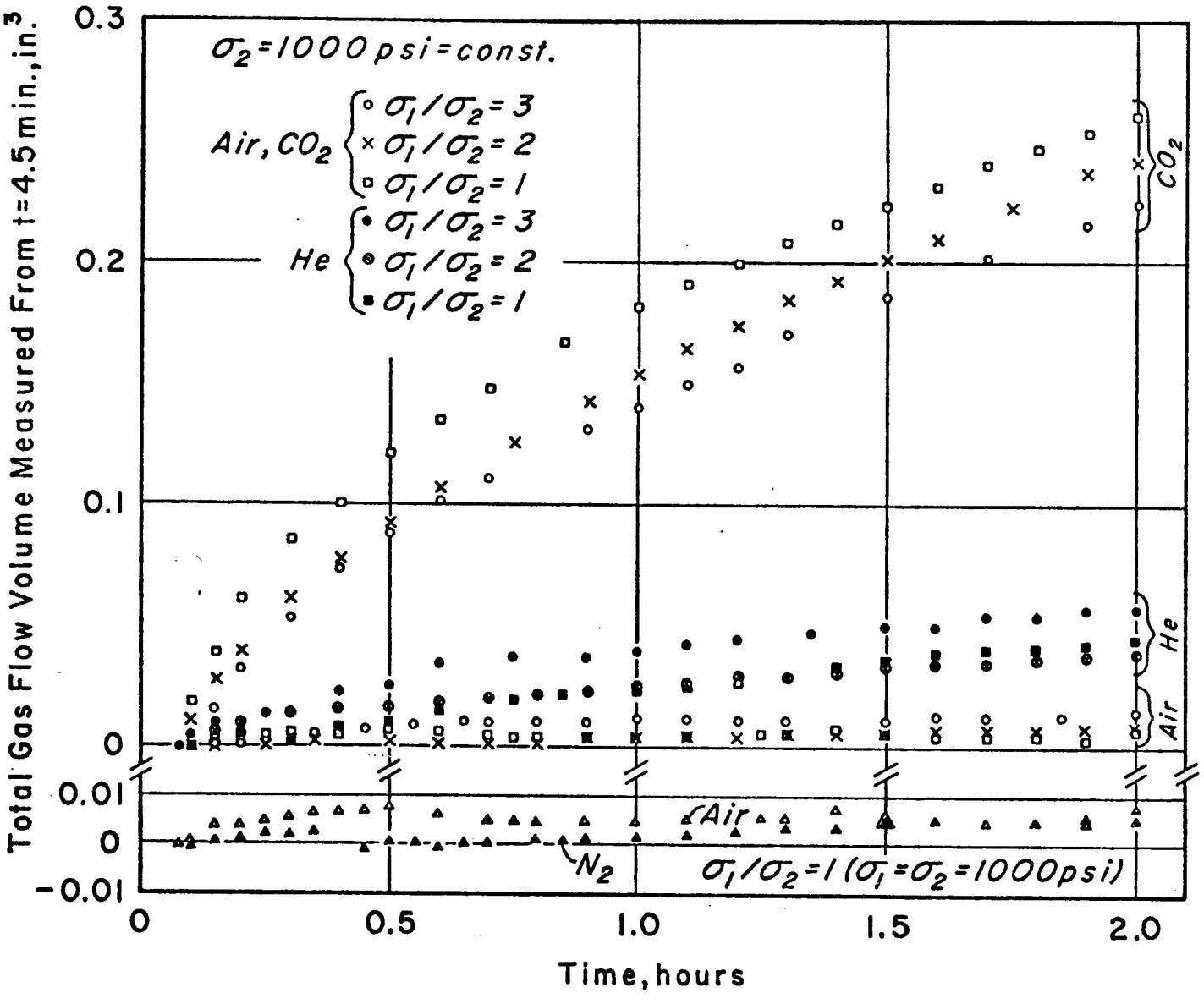

Fig. 11. Apparent Absorption Curves for Various Gases and Stress Ratios at σ_2 = 1000 psi = constant. (Constant Internal Pressure)

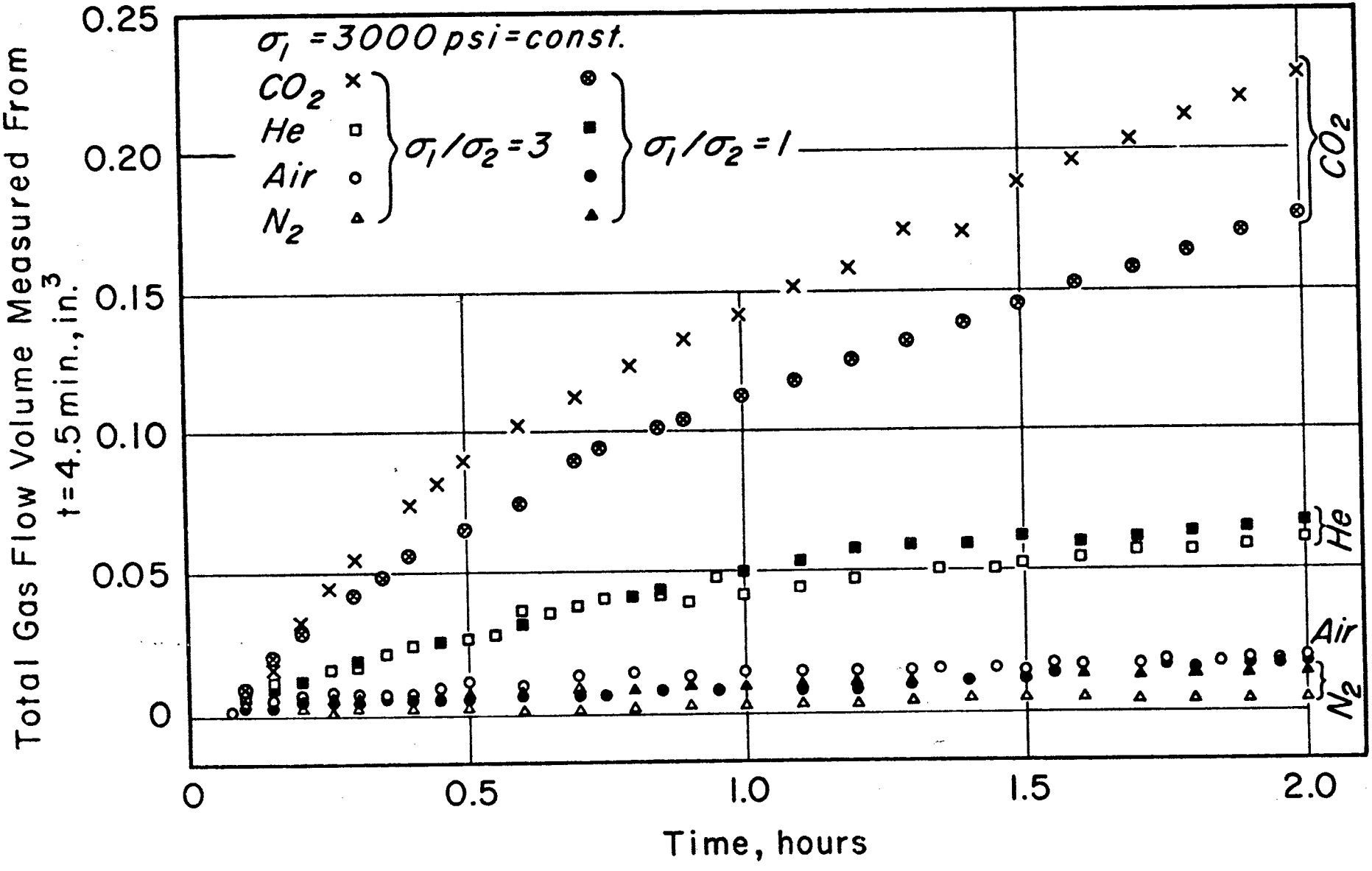

Fig. 12. Apparent Absorption Curves for Various Gases at σ_1/σ_2 = 1 and 3 for σ_1 = 3000 psi

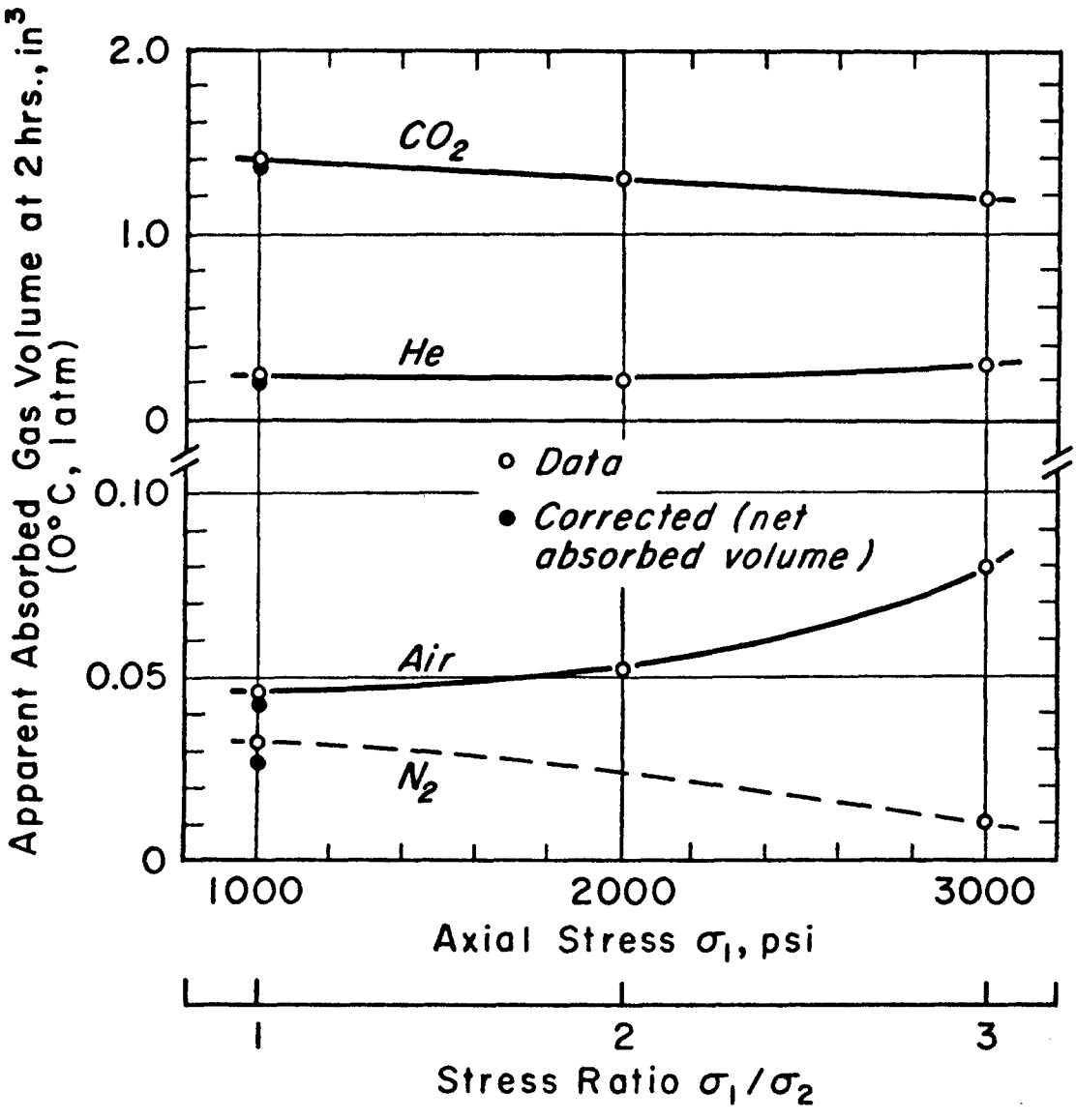

Fig. 13. Apparent Absorbed Gas Volume versus Axial Stress σ_1 at σ_2 = 1000 psi = constant (Constant Internal Pressure). Volumes adjusted to 0°C and 1 atmosphere.

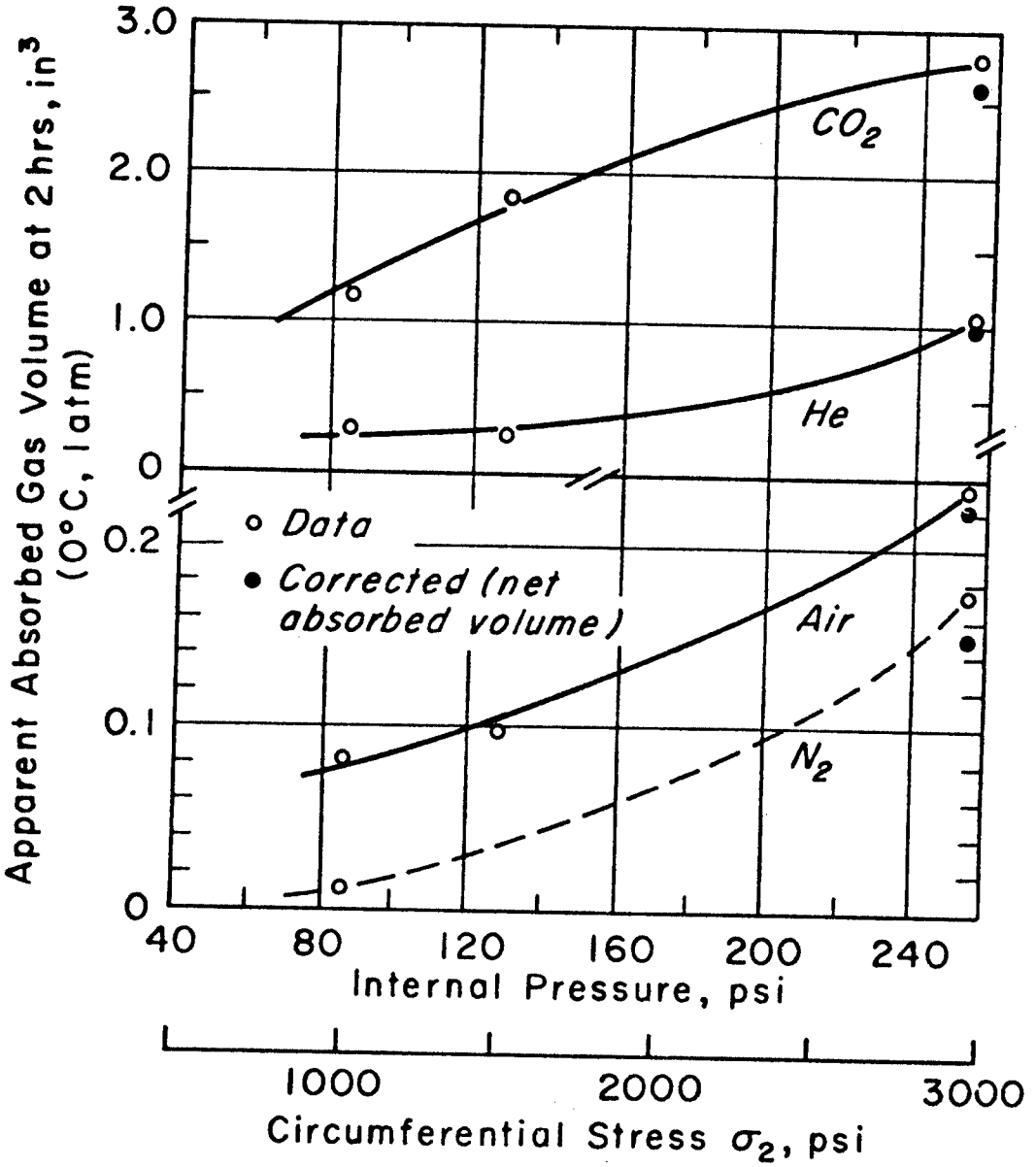

Fig. 14. Apparent Absorbed Gas Volume versus Internal Pressure (σ_1 = 3000 psi = constant). Volumes adjusted to 0°C and 1 atmosphere.

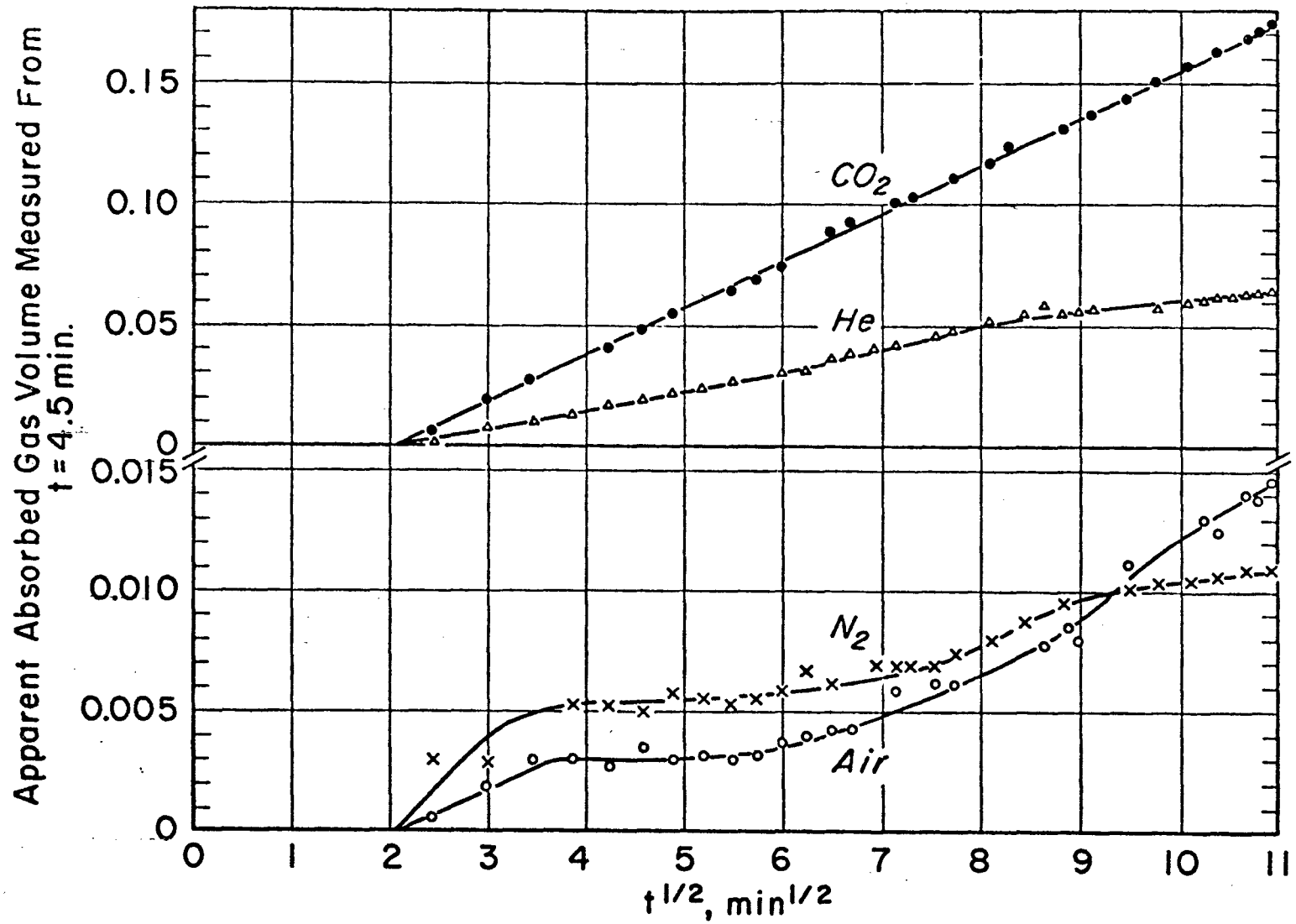

Fig. 15. Apparent Absorption Curves for Various Gases under Creep Conditions at $\sigma_1/\sigma_2 = 1$ ($\sigma_1 = \sigma_2 = 3000$ psi)

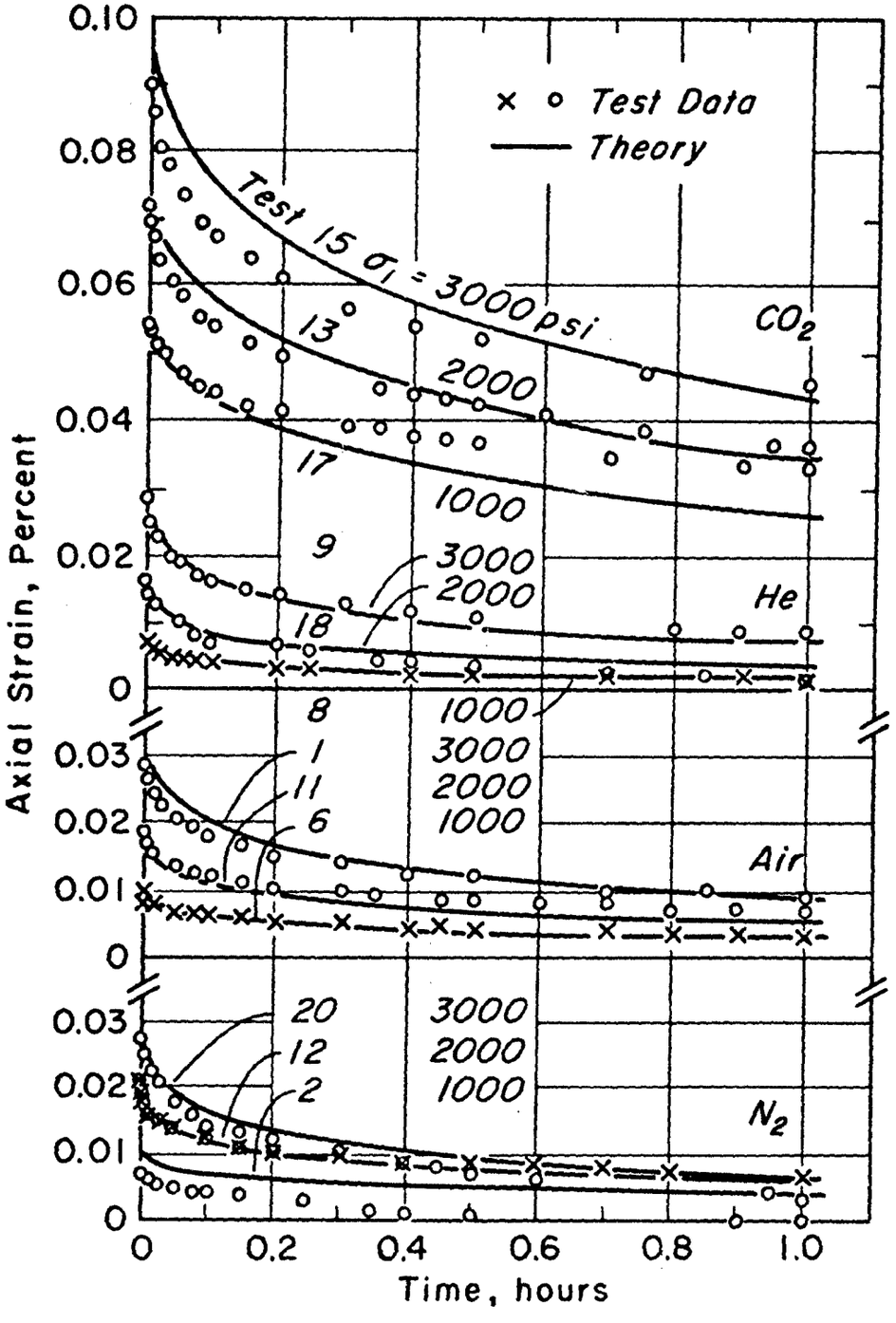

Fig. 16. Recovery Curves Following Creep for Two Hours at σ_2 = 1000 psi and Various Values of σ_1